

## Chapter 3

### Experimental Details

#### 3.1. Material preparation

##### 3.1.1. Vacuum arc melting

High purity elemental pieces of Ni (99.99%), Fe (99.99%), Cr (99.9%), Si (99.999%), and B (99.7%) are procured from Alfa Aesar were used for preparation of master alloy ingots. The master alloy of nominal composition  $(\text{Ni}_{87}\text{Fe}_4\text{Cr}_9)_{78}\text{Si}_8\text{B}_{14}$  was produced using high purity elements through inert vacuum arc-melting technique (**Figure 3.1**). Prior to melting, the chamber was evacuated to a vacuum of  $10^{-2}$  bar and purged with high-purity argon gas. This evacuation backfilling cycle was repeated twice to ensure a low oxygen environment during melting.



Figure 3.1- (a) Vacuum Arc Melting facility for Ingot preparation and (b)-(c) prepared master alloy ingots.

To compensate for the potential loss of phosphorus due to its volatility under arc melting conditions, an additional 3 wt% of phosphorus was added to the charge. Arcing was initiated in a partially argon-filled chamber to begin melting the elemental constituents. The master alloy ingots were re-melted multiple times to ensure thorough homogenization of the alloy.

### 3.1.2. Amorphous Electrical ribbon preparation

Amorphous alloy ribbons were synthesized via rapid solidification using an in-house melt-spinning setup operated under ambient conditions.



Figure 3.2- Melt spinning facility for preparation of Amorphous Electrical Steel.

Chill block melt spinning (CBMS) for producing narrow-width ribbons and planar flow melt spinning (PFMS) for wider ribbon fabrication were employed. The pre-weighed alloy ingot was placed in a quartz crucible with a bottom nozzle, and melting was performed using a water-cooled RF induction coil. Inert gas pressure was applied from above to facilitate melt ejection as shown in **Figure 3.2**. As the molten alloy was expelled, it impinged on the surface of a rotating metallic wheel, resulting in the formation of continuous amorphous ribbons of 25 mm width and average ribbon thickness of  $\sim 28 \mu\text{m}$  (**Figure 3.3a-b**). The melt-spun ribbons are bendable and exhibit metallic lustre (**Figure 3.4**). Process parameters were carefully optimized to ensure the desired ribbon quality. The selected alloy composition was prepared using commercially available raw materials through the planar flow casting route, yielding ribbons with varying thicknesses suitable for further characterization.

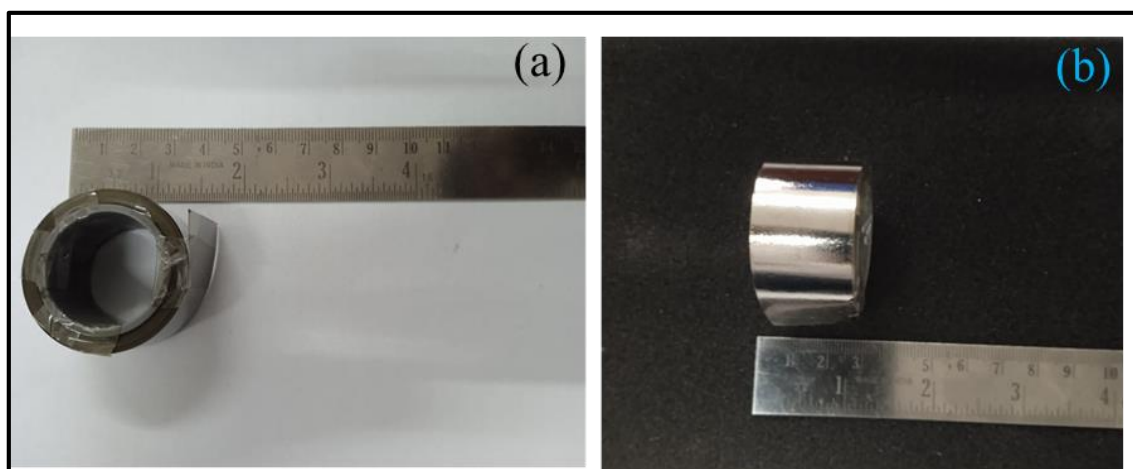


Figure 3.3- (a) Amorphous Electrical steel ribbons prepared through the melt spinning technique. (b) Amorphous Ribbon role.

### 3.1.3. Surface modification of Amorphous Electrical ribbons

The precursor ribbons were cut into rectangular samples with a cross-sectional area of  $20 \times 10 \text{ mm}^2$  and then underwent surface modification through potentiostatic cathodic

corrosion to create electrochemically active surface phases. The chronoamperometric method for the corrosion of the ribbon surface was carried out in a 1 M KOH electrolyte at a potential corresponding to 10 mA/cm<sup>2</sup> (hydrogen generation regime) with a scan rate of 20 mV s<sup>-1</sup>. To study the impact of corrosion time on catalytic performance, the corrosion duration was systematically varied to 0, 30, 45, 60, 90, and 120 minutes, respectively. The electrode samples are labelled as S0, S30, S45, S60, S90, and S120 to indicate the different modification times used in this thesis. These corroded ribbon electrodes were thoroughly washed with deionized water, ethanol, and dried at room temperature.

In a similar way, master alloy produced with composition of (Ni<sub>87</sub>Fe<sub>4</sub>Cr<sub>9</sub>)<sub>78</sub>Si<sub>8</sub>B<sub>14</sub> was cut into ribbons with a size of (20 × 10 mm<sup>2</sup>) and were chemically de-alloyed in presence of 0.5 M HNO<sub>3</sub> for different time periods from 0–120 minutes to optimize electrocatalytic performance. Post acid treatment, these electrode ribbons were rinsed with deionized water and dried under vacuum and then subsequently used for Hydrogen generation, OER and Methanol fuel cell studies.

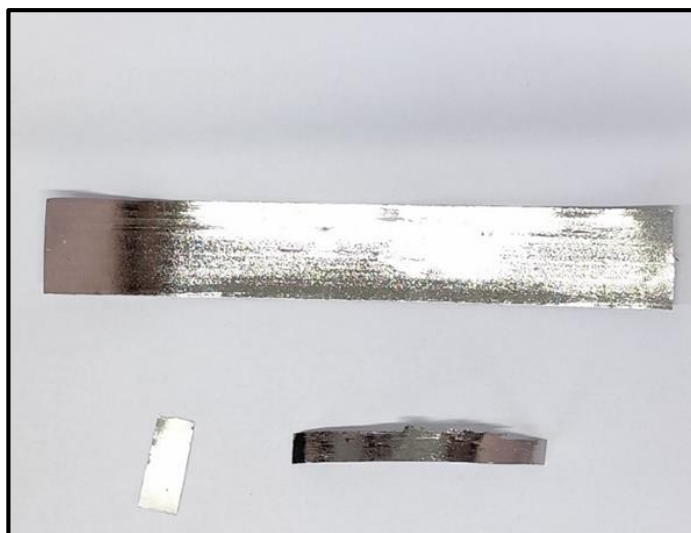


Figure 3.4- Top view of Melt spun amorphous electrical steel ribbons for electrocatalysis.

### 3.1.4. Electro chemical work station

An electrochemical workstation, commonly referred to as a potentiostat, is a vital analytical instrument used in electrochemical research. It allows precise control and monitoring of electrical potentials and currents in electrochemical systems, making it essential for studying reaction mechanisms, material performance, and electrochemical energy devices. A potentiostat typically operates using a two- or three-electrode configuration, comprising of working electrode (WE), Counter Electrode (CE) and Reference Electrode (RE) (**Figure 3.5**).

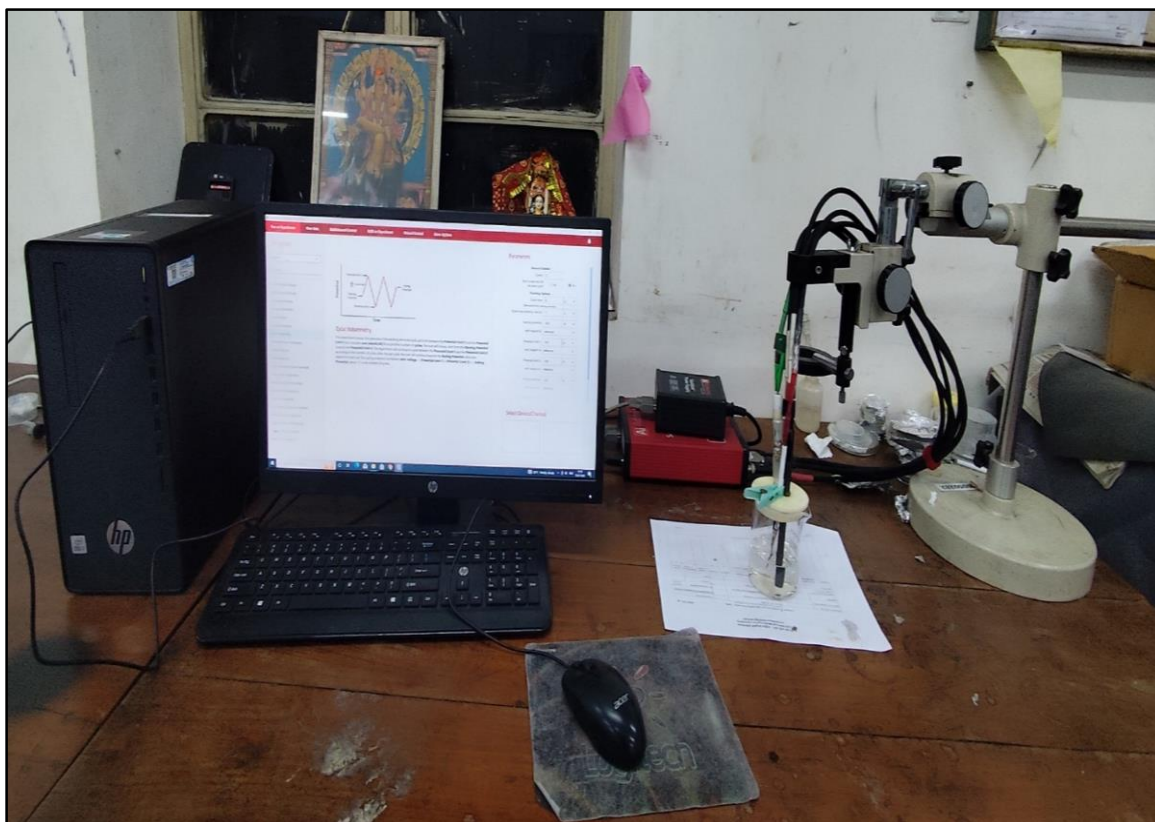


Figure 3.5- Electrochemical cum Electrical Potentiostat/ Galvanostat work station.

Working electrode at which the electrochemical reaction of interest takes place. It is typically made from materials like glassy carbon, gold, platinum, or modified substrates. The WE is central to studying the catalytic behavior of materials. Counter electrode completes the circuit by allowing current to flow from the working electrode. Common materials for the counter electrode include platinum mesh, platinum wire, or graphite, which are chemically inert and conductive. The reference electrode (RE) provides a stable and known reference potential against which the potential of the working electrode is measured. Depending on the electrolyte environment, electrodes such as Ag/AgCl, Hg/HgO, or Saturated Calomel Electrode (SCE) are used. The choice of reference electrode is crucial and depends on the pH and composition of the electrolyte solution.

Electrochemical workstations are highly versatile and support a range of experimental techniques for fundamental and applied electrical and electrochemical studies. Common applications include Cyclic Voltammetry, Linear Sweep Voltammetry (LSV), Electrochemical Impedance Spectroscopy (EIS), Chronoamperometry (CA), Chronopotentiometry (CP) and Differential Pulse Voltammetry (DPV). Due to its multifunctional capabilities, the electrochemical workstation plays a critical role in the development and characterization of materials for Fuel cells, Batteries and super-capacitors, Water splitting and hydrogen production, Electrocatalysts (for HER, OER, ORR, etc.) and Chemical and biosensors.

### 3.1.5. Chemicals and Reagents

Potassium hydroxide (KOH) and Methanol (ACS reagent grade,  $\geq 99.8\%$ ) were sourced from SRL India and Merck (Sigma-Aldrich), respectively. A range of KOH solutions with varying molar concentrations was prepared using deionized water to obtain electrolytes with different pH values (**Figure 3.6**). These electrolytes were employed to

evaluate their effectiveness in water splitting, specifically focusing on the oxygen evolution reaction (OER) for hydrogen generation.

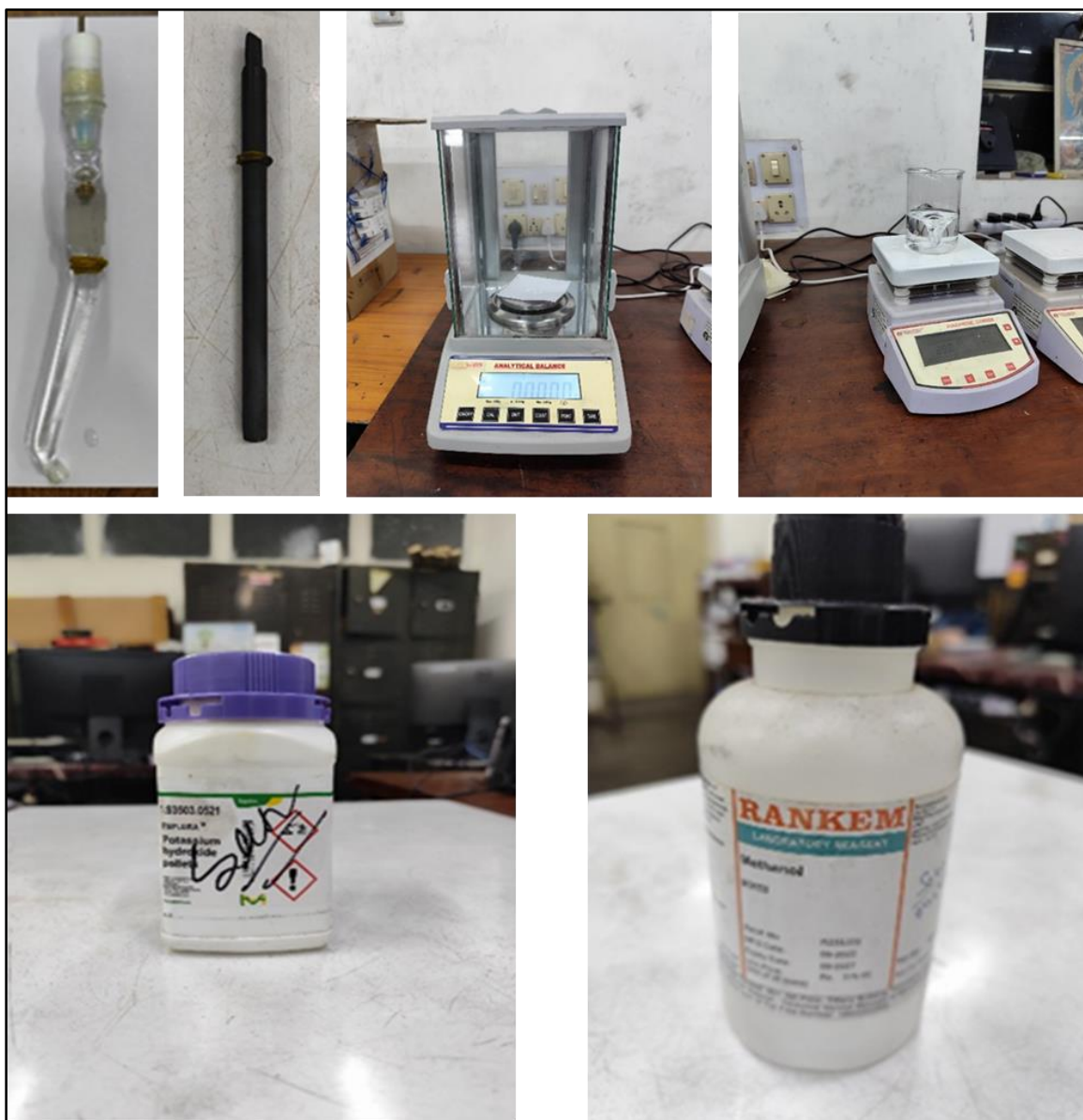


Figure 3.6- Images of Reference electrode, Weighing machine, Stirrer machine, KOH and Methanol chemicals.

For methanol fuel cell studies, an electrolyte solution comprising 1 M methanol in the presence of 1 M KOH was prepared. This alkaline medium was utilized to investigate the

methanol oxidation reaction (MOR) and evaluate the electrocatalytic performance of the electrode materials under fuel cell operating conditions.

## 3.2. Material Characterization

### 3.2.1. X-Ray diffraction (XRD) analysis

X-ray diffraction (XRD) analysis was carried out to examine the structural and phase characteristics of both as-quenched and surface treated samples. The measurements were performed using a Bruker D8 Discover diffractometer equipped with Cu-K $\alpha$  radiation, operating in Bragg-Brentano geometry.

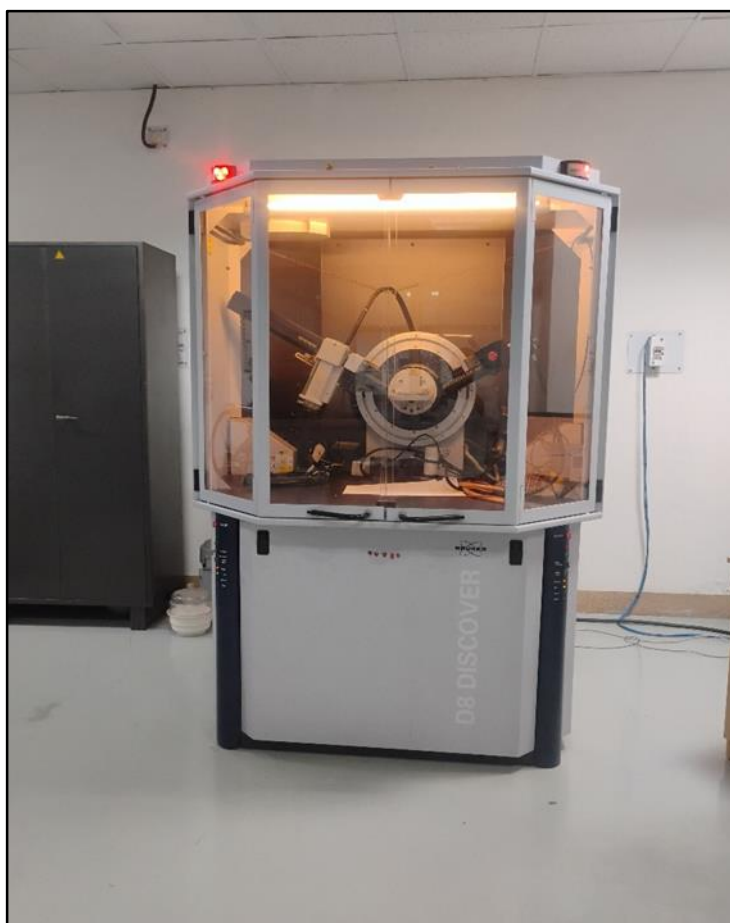


Figure 3.7- X-Ray diffraction (XRD) analysis facility for Elemental phase analysis.

Data acquisition was controlled via the XRD Commander software, using a step size of  $0.02^\circ$  and a scan speed ranging between 0.8 to 0.9. For sample preparation to XRD, ribbon specimens were affixed onto glass slides using a thin double-sided adhesive tape, and the air-exposed surface of the ribbons was primarily analysed. The collected diffraction patterns were subsequently processed and interpreted using EVA Diffrac software for phase identification. Further analysis, including peak broadening and area integration, was carried out using Origin software to estimate parameters such as average crystallite size ( $D$ ) and crystalline volume fraction ( $V_{cr}$ ) (**Figure 3.7**).

### 3.2.2. Transmission electron Microscopy



Figure 3.8- Transmission electron Microscopy facility for material characterisation.

TEM specimens were prepared using a combination of electrolytic twin-jet polishing and ion-milling techniques. Initially, 3 mm diameter discs were punched from the ribbon samples using a diamond anvil punch. Due to the high flexibility and mechanical strength of the as-quenched ribbons, burrs were often observed along the edges, which were carefully removed by mechanical edge grinding.

Subsequently, the punched discs were mechanically thinned on both sides using 4000-grit emery paper (Buehler, USA) to achieve the desired thickness. Special care was taken to minimize heat generation due to friction during the thinning process. The pre-thinned disc was then mounted on the Struers twin-jet polishing holder for further electrolytic thinning prior to TEM observation. Detailed analysis of phase composition, nano-structural features, and crystallographic orientation was carried out using analytical transmission electron microscopy (TEM) on a Philips CM200, and high-resolution TEM (HRTEM) on a JEOL 2200FS, both operated at an accelerating voltage of 200 kV as shown in **Figure 3.8**.

### **3.2.3. Scanning Electron Microscopy**

The surface morphology and composition of catalysts were examined using scanning electron microscopy (SEM) equipped with an energy-dispersive X-ray spectrometer (EDS), Make: Oxford Instruments as shown in **Figure 3.9**. For sample preparation to SEM, ribbon specimens were affixed onto glass slides using a thin double-sided adhesive tape, and gold coated. The face exposed surface of the ribbons was primarily analysed. energy-dispersive X-ray spectrometer (EDS) was used to evaluate the elemental mapping at point and bulk sample basis. Matrix homogeneity was assessed using the backscattered electron imaging mode, while quantitative elemental distribution was evaluated through line scans and area mapping using a wavelength dispersive spectroscopy (WDS) detector.



Figure 3.9- Scanning Electron Microscopy facility for material characterisation.

#### 3.2.4. X-ray Photoelectron Spectroscopy

The X-ray photoelectron spectroscopy (XPS) spectra of the ribbon samples were obtained through ESCALAB 250Xi & Thermo-Fisher as shown in **Figure 3.10**. It is a surface-sensitive analytical technique used to identify the chemical species and electronic states of the elements present on the developed electrode material, especially upon the material surface, which primarily participates in the catalytic activity.

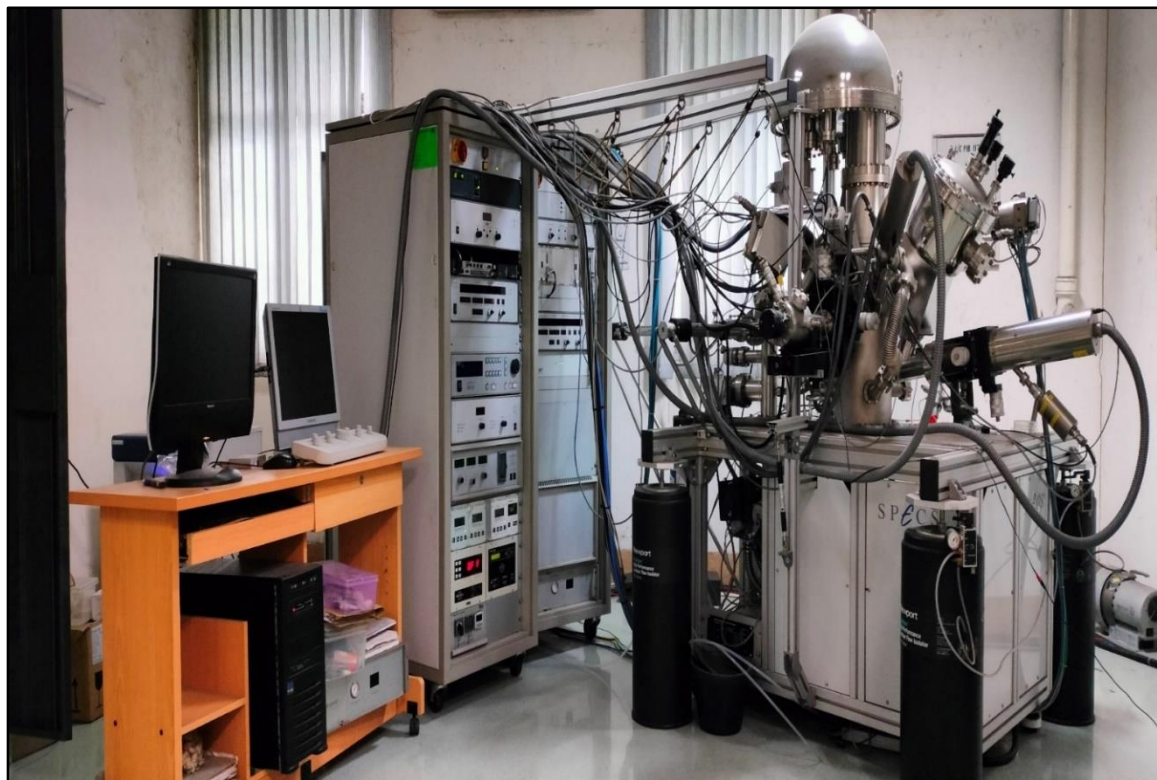


Figure 3.10- X-ray Photoelectron Spectroscopy for surface analysis.

### 3.3. Solar photo voltaic plant

A 500 kWp solar photovoltaic (PV) plant was designed and installed to assess key parameters involved in PV system design. Section photograph of Solar Photo-Voltaic plant along with installed Inverter unit is shown in **Figure 3.11**. The design process considered various factors such as available site area, historical solar irradiance data, optimal tilt angle, structural assessment of the building, and shadow analysis.

Design evaluation was also carried out based on energy output, capacity factor, and performance ratio of the plant. PVSYST© V6.63 software was employed for simulation

and system design. Additionally, the installed PV system serves as a platform for conducting life cycle assessment studies.

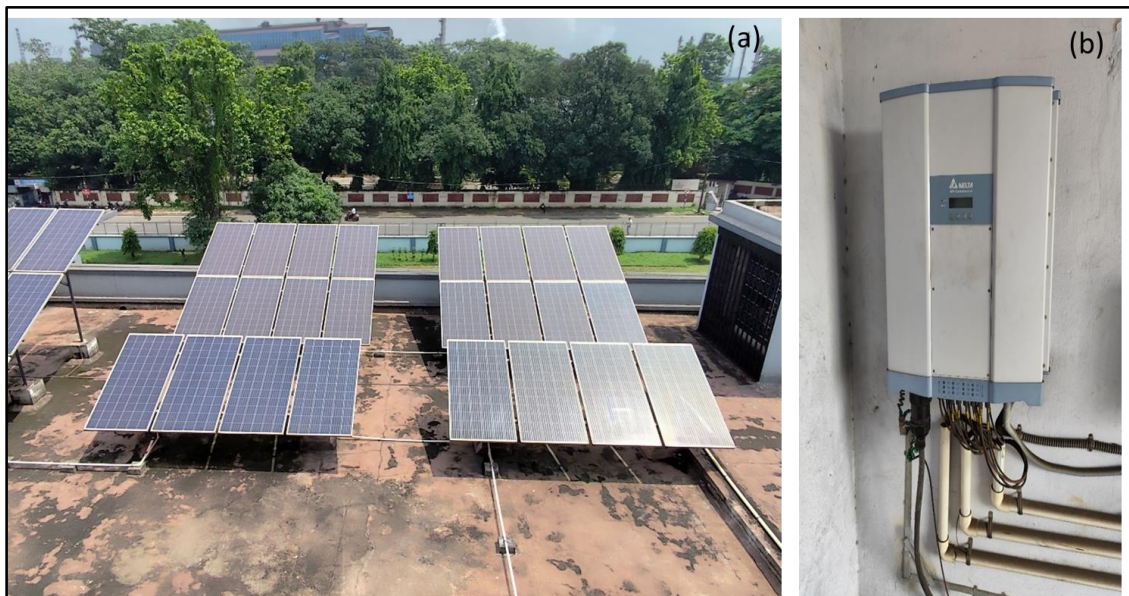


Figure 3.11- (a) Section photograph of Solar Photo-Voltaic plant (b) Inverter panel.